Wang R, Tan Q, Jin H, et al. Characteristics of the interferon regulatory factor IRF5 and its stimulation expression by *Elizabethkingia miricola* Infection in black-spotted frog (*Pelophylax nigromaculatus*). *Israeli Journal of Aquaculture - Bamidgeh*. 2023;75(1):1-13. doi:10.46989/001c.77752

Original Research Articles

Characteristics of the interferon regulatory factor IRF5 and its stimulation expression by *Elizabethkingia miricola* Infection in black-spotted frog (*Pelophylax nigromaculatus*)

Ronghua Wang[1], Qing Tan[2], Hongchun Jin[3], Ke Li[1], Menglu Yan[1], Yan Kang[1], Shuqiong Li[1], Jinlong Wang[1], Pinhong Yang[1a], Zhongyuan Chen[1b]

[1] Hunan Provincial Key Laboratory for Health Aquaculture and Product Processing in Dongting Lake Area, Hunan Provincial Key Laboratory for Molecular Immunity Technology of Aquatic Animal Diseases, College of life and environmental sciences, Hunan University of Arts and Science, Changde, Hunan 415000, China, [2] Changde Vocational Technical College, Changde 415000, China, [3] Anxiang County Science and Technology Bureau, Changde 415600, China

Keywords: Elizabethkingia miricola, Interferon regulatory factor 5 (IRF5), molecular function, Pelophylax nigromaculatus

https://doi.org/10.46989/001c.77752

Israeli Journal of Aquaculture - Bamidgeh

Vol. 75, Issue 1, 2023

Interferon regulatory factors (IRFs) have been confirmed as vital transcription factors for the immune system, which play a certain role in anti-infection defense, immune regulation, hematopoietic cell development, and maturation of the immune system. In this study, the cDNA of Interferon regulatory factor 5 (IRF5) was cloned from black-spotted frog, *Pelophylax nigromaculatus*, and termed PnIRF5. The results indicated, the full-length cDNA of PnIRF5 was 2090 bp, and a putative protein of 504 amino acids was encoded. The results of protein domain prediction suggested that PnIRF5 exhibited a DNA-binding domain (DBD), a middle region (MR), an IRF association domain (IAD), a virus activated domain (VAD), as well as two nuclear localization signals (NLSs). Phylogenetic analysis clustered PnIRF5 into the amphibian IRF5 subgroup in vertebrate IRF5 group. The results of qPCR show that PnIRF5 mRNA was expressed in all examined tissues, with higher levels were identified in the kidney, intestine, and lung. The gene expression of PnIRF5 was analyzed in kidney, spleen, and liver of black-spotted frog after challenged with *Elizabethkingia miricola*, and the maximum expression level of PnIRF5 in liver, spleen, and kidney were 1.80, 2.33 and 2.88 times that at 0 days post challenged, respectively. As indicated by the results, the PnIRF5 protein may take on critical significance in protecting black-spotted frog from *E. miricola* infection, and they may play a certain role in the immune response of black-spotted frog against bacteria.

INTRODUCTION

Interferon regulatory factors (IRFs) serve as critical transcription factors that play a certain role in immune cell apoptosis and differentiation, organism defense against pathogens.[1,2] IRF family comprise nine members in mammalian. To be specific, IRF1-9 and a total of 11 members are identified in fish IRF family, except for IRF1~9, IRF10, as well as IRF11.[3] IRF10 was first identified in birds, and it was later reported only in fish and birds, whereas IRF11 was only identified in fish.[4-7]

IRF5, member of IRFs, has been reported as a vital transcription factor mediating innate immune response while bridging adaptive immunity. IRF5 has been demonstrated with profound and diverse regulatory roles in the expression of inflammatory factors, macrophage polarization, B lymphocyte activation and proliferation, plasma cell differentiation, as well as antibody secretion.[8-12] In innate immune response, IRF5 exerts vital regulatory effects in regulating downstream immune responses of pattern recognition receptor (PPRs) pathway (e.g., Toll like receptor (TLR) 3, TLR4, TLR7, TLR9, nucleotide-binding oligomerization domain 2 (NOD2), as well as retinoic acid inducible gene I (RGI-I)).[13-15] Similar to other IRF family members, IRF5 predominantly resides in the cytosol in a latent form as a monomer in unstimulated cells. IRF5 stimulated by viruses, bacteria, or mutant cells are phosphorylated, homo/hetero-dimerized and then translocated from cytoplasm into the nucleus to modulate the production of cytokines, chemokines, and interferons.[2,6,14] Extensive research has been conducted on the gene structure and

a * Corresponding author. emial: yphong@huas.edu.cn (P.Y.)

b * second Corresponding author. e-mail: Chenzy@huas.edu.cn (Z. C.)

function of IRF5 in Mammalia, Aves, and Fish,[2,16] whereas IRF5 in amphibian has been scarcely investigated.

The black-spotted frog, *Pelophylax nigromaculatus*, belongs to *Pelophylax*, *Ranidae,* extensively distributed in east Asia.[17] Since the success of rearing, it on an artificial diet, black-spotted frog has been widely farmed in China due to its growing fast, delicious, and nutritious, taking on great economic significance. However, a considerable number of black-spotted frogs in farms in Hunan Province in south-central China have been subjected to an epidemic meningitis-like disease (i.e., "frog torticollis" or "frog cataract") since 2016.[18,19] epidemic meningitis-like disease brings high lethality to frogs in several days, which is one of the greatest threats to the health of frogs and its industry.[18-20] *Elizabethkingia miricola* was identified as the pathogen to the disease.[19-21] The black-spotted frog, a type of vertebrate, has evolved powerful immune system, which comprises innate immune system and adaptive immune system.[22,23]

The investigation of the immune factors involved in the frog resistance to *E. miricola* infection and their function can provide basic data for the development of novel methods of preventing epidemic meningitis-like disease. To gain more insights into the role of IRF5 in black-spotted frog resistance to *E. miricola* infection, the *Pn*IRF5 was cloned in this study, and its patterns of tissue expression in response to *E. miricola* challenge was studied through quantitative real-time PCR (qPCR).

MATERIALS AND METHODS

ANIMALS AND BACTERIUM SOURCES

Healthy cultured black-spotted frogs weighing 35±5 g originated from a commercial aquaculture farm in Changde (Hunan, China). Black-spotted frogs were kept in two 1 m×1 m×0.6 m canvas pool to adapt for two weeks prior to experiment. The respective black-spotted frog was fed 3-5 *Tenebrio molitor* twice daily at 08:00 a.m. and 16:00 p.m. No mortality was identified prior to experiment, and all selected experimental frogs were euthanized with MS-222(Sigma-Aldrich, Germany) before sampling. *E. miricola* was isolated and identified from black-spotted frogs infected with torticollis disease in Changde.

TOTAL RNA EXTRACTION AND CDNA SYNTHESIS

Total RNA from each sample (approximately 100 mg) was extracted with the Trizol reagent (Invitrogen, Carlsbad, CA, USA) in accordance with the manufacturer's instructions. Total RNA purity and concentration were examined with spectrophotometer (Eppendorf Bio Spectrometer® basic, Germany), and the integrity was examined by electrophoresis with 1% agarose gel. Only intact RNA samples with 260/280 nm ratio between 1.8 and 2.0 were employed for cDNA synthesis. cDNA synthesis was carried out using Revert Aid™ First Strand cDNA Synthesis Kit (ThermoFisher, Carlsbad, CA, USA) following the method recommended by the manufacturer.

IRF5 CDNA CLONING

Based on the transcriptome sequencing of black-spotted frogs, specific primers of IRF5 were designed (**Table 1**) with Primer Premier 6.0 and synthetized by Sangon Biotech Co., Ltd. (Wuhan, China). The middle sequence of *Pn*IRF5 was obtained with primer pairs PnIRF5-1F/PnIRF5-1R and PnIRF5-2F/PnIRF5-2R (**Table 1**). The PCR amplifications were performed with 1 cycle at 95 °C for 5 min, 30 cycles at 95 °C for 30 s, 56 °C for 45s, as well as 72 °C for 60s. Subsequently, the samples were subjected to a final extension step at 72 °C for 10 min and then stored at 16°C.

The 5'-end and 3'-end cDNA fragments of *Pn*IRF5 gene were amplified with 5'-RACE kit (Sangon, Shanghai, China) and 3'-RACE kit (Sangon, Shanghai, China) in accordance with the method recommended by the manufacturer, respectively. The respective amplified PCR product was examined with 1% agarose gel that was stained with GelGreen (Biosharp, Hefei China). Furthermore, the target DNA fragments were purified with FastPure Gel DNA Extraction Mini Kit (Vazyme, Nanjing, China) and then cloned into pUCm-T Vector (Sangon, Shanghai, China) for sequencing at Sangon biotech Co., Ltd (Wuhan, China).

SEQUENCE ANALYSIS

Sequence assembly was obtained based on the SeqMan module of DNAStar 7.0.1 software. The sequence homology of *Pn*IRF5 was investigated using the BLAST algorithm on the website of National Center for Biotechnology Information (http://www.ncbi.nlm.nih.gov/blast). The amino acid sequences were translated with the Translate tool of Expert Protein Analysis System (https://web.expasy.org/translate/). The conserved domain of *Pn*IRF5 was predicted with Simple Modular Architecture Research Tool (http://smart.embl-heidelberg.de/). Multiple sequences were aligned using Clustal X2.1 and then visualized with GeneDoc 3.2. The 3D structure of *Pn*IRF5 was predicted by Robetta (https://robetta.bakerlab.org/) and visualized by PyMOL 2.5.2. The neighbor-joining (NJ) method was used to build a phylogenetic tree with 1000 bootstrap replicates using MEGA 11 software.

TISSUE SPECIFIC PNIRF5 EXPRESSION PROFILES

Spleen, intestine, liver, muscle, brain, kidney, lung, and stomach were taken from three health black-spotted frogs, respectively. The method of RNA extraction and cDNA synthesis followed the above description. The qPCR reaction was performed using the Roche LightCycler480 II (Roche, Basel Switzerland). The putative housekeeping gene 18S was amplified as an internal control for cDNA normalization with the primer set 18S-RTF/18S-RTR (**Table 1**). IRF5 gene expression was detected using the primer set PnIRF5-RTF/ PnIRF5-RTR (**Table 1**). The qPCR reaction system comprised 9.2 µL of the cDNA sample that was diluted with 8 times the volume with nuclease-free water, 10 µL of ChamQ Universal SYBR qPCR Master Mix (Vazyme, Nanjing China), and 0.4 µL of the respective gene specific primer (10 µmol/L). The qPCR cycling protocol covered 1

Table 1. Primer sequences used in this study.

Primer	Sequence (5'-3')
Gene cloning	
PnIRF5-1F	AGTCATCGTCTTGGAAGTG
PnIRF5-1R	CGTCTCAAGGCTGAATAGT
PnIRF5-2F	ACAGTAACCTTGAGCCAAC
PnIRF5-2R	CTACAGTCAGATGAAGTAACAC
3'RACE	
PnIRF5-3'out	AGTCCACAGATGCTGCCATTGACTGACCT
PnIRF5-3'in	AACCTTGAGCCAACCCCAGAGCAAGTGGA
5'RACE	
PnIRF5-5'out	GGACTAATGAGTAAGCCTGGAATCCCCT
PnIRF5-5'in	TGCCTTCCACTTTGCAGGGTCAGGTTC
Primers for fluorescence quantitative PCR analysis	
PnIRF5-RTF	CCAGGCTTACTCATTAGTCCAC
PnIRF5-RTR	CAAACAGCTCCACTTGCTCT
18S-RTF	CGTTGATTAAGTCCCTGCCCTT
18S-RTR	GCCGATCCGAGGACCTCACTA

cycle of 95 °C for 10 min, 40 cycles of 95 °C for 10 s, 60 °C for 10 s, as well as 72 °C for 15 s, followed by a dissociation curve analysis to verify the amplification of a single product. The temperature was elevated from 65 to 95 °C with an increment of 0.5 °C per 5 s, and the data were analyzed using the $2^{-\Delta\Delta Ct}$ method. Furthermore, the results were plotted using GraphPad Prism 6.

EXPRESSION PROFILES OF PNIRF5 MRNA AFTER E. MIRICOLA INFECTION

Activated *E. miricola* were incubated at 28 °C for 24 h in brain heart infusion (BHI) broth. The cells were cleaned with sterile PBS and then resuspended in PBS to 1×10^8 CFU (colony forming unit)/mL. The respective black-spotted frog was intraperitoneal (i.p.) injection with 200 μL live *E. miricola*. The room temperature was maintained at 28 ± 1 °C in the experimental process. Black-spotted frog spleen, liver, and kidney samples were collected at 0-, 1-, 2-, 3-, and 4-days post injection. The method of RNA extraction and cDNA synthesis followed the above description. The mRNA transcription levels of *Pn*IRF5 were determined through qPCR in accordance with the previous description.

STATISTICAL ANALYSIS

All data were expressed as mean ± SD from separate experiments. All statistical analysis was conducted using SPSS Version 25.0 (SPSS Inc., Chicago, IL, USA). The one-way ANOVA and Duncan's MRT was employed for between group comparisons. A probability level of $p < 0.05$ indicated a difference with statistical significance.

RESULTS

MOLECULAR CHARACTERIZATION OF PNIRF5

The full-length cDNAs of black-spotted frog IRF5 comprised 2090 bp. The *Pn*IRF5 cDNA (GenBank accession no. OP039101) contained a 356 bp 5'-untranslated region (UTR), a 219 bp 3'-UTR, and an ORF of 1515 bp that was translated into a 504 amino acid putative peptide with a predicted molecular mass of 56.9 kDa. No mRNA instability motifs (ATTTA) and polyadenylation signals (AATAAA) were upstream of the polyA tail (**Figure** S1). The *Pn*IRF5 covered the conserved domains as follows: a DNA-binding domain (DBD, 1-104 aa), a middle region (MR, 108-195 aa), an IRF association domain (IAD, 196-327 aa), a virus activated domain (VAD, 326-479 aa), as well as two nuclear localization signals (NLSs, 5-10 aa, 413-419 aa) (**Figure 1**, **Figure S1**).

As indicated by the BLAST analysis results, *Pn*IRF5 matched significantly with IRF5s from other species. The IRF5 from *Rana temporaria* (GenBank no: XP_018412577.1) shared the maximum identity (93.85%) with *Pn*IRF5. Besides, *Pn*IRF5 exhibited high identity with other amphibians (e.g., 90.10% identity with *Nanorana parkeri* (GenBank: XP_018412577.1) and 80.79% identity with *Engystomops pustulosus* (GenBank: KAG8576680.1)). For Six IRF5s from other species using in multiple sequence alignment, *Pn*IRF5 exhibited the maximum overall similarity (61.26%) to the homolog from *Mauremys mutica*, exhibiting 83.81% similarity in the DBD and 66.09% similarity in the IAD (**Table S1**).

PHYLOGENETIC TREE ANALYSIS

To gain insights into the evolutionary relationships, a phylogenetic tree was built using the NJ method with 1000 bootstrap tests based on the multiple alignments of the

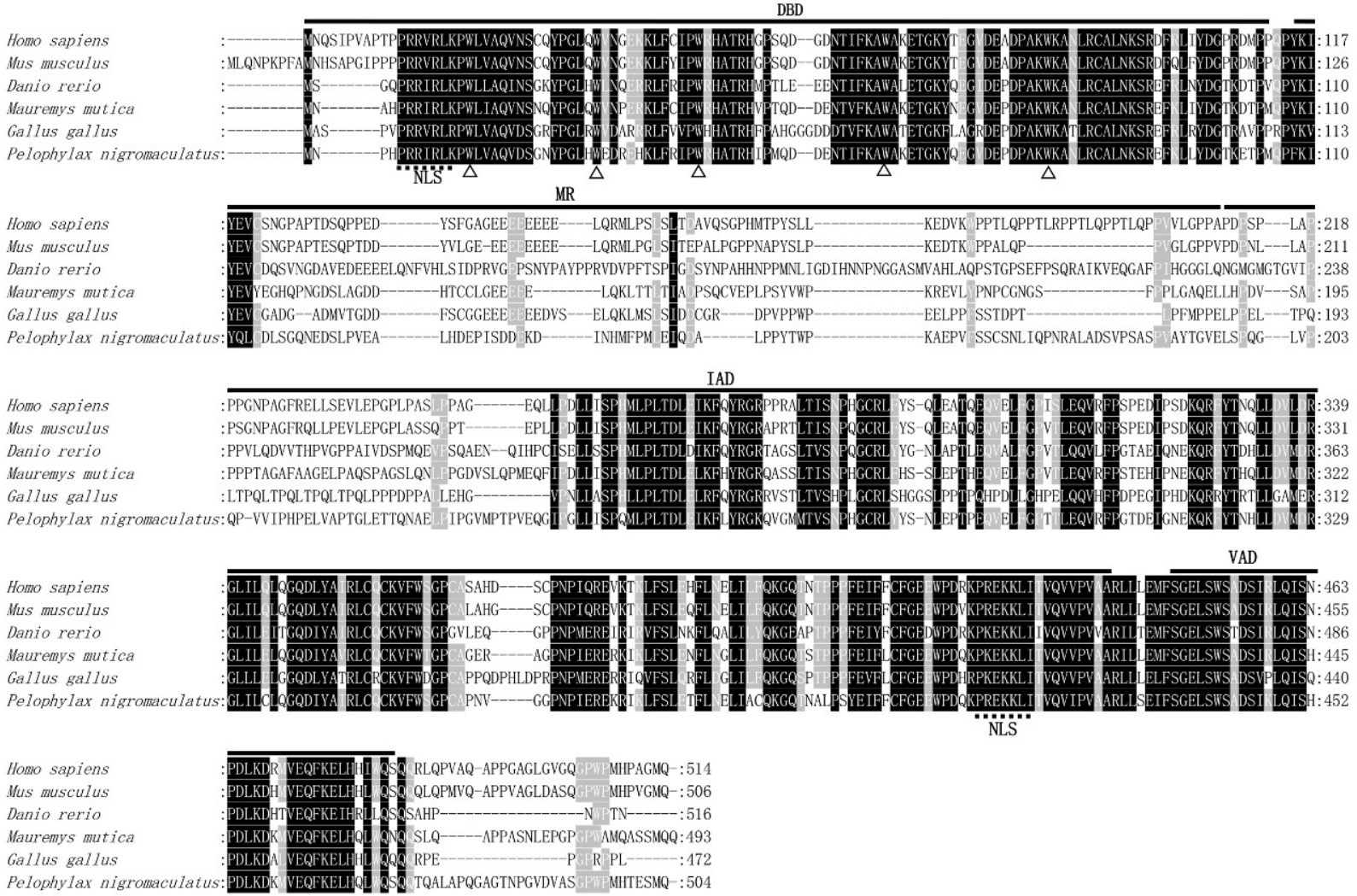

Figure 1. Alignment of amino acid sequences of *Pn*IRF5 and other known IRF5s.

Evolutionary conserved amino acid sequences are highlighted in black. The predicted DNA binding domain (DBD), middle region (MR), IRF association domain (IAD) and virus activated domain (VAD) were indicated by lines above the aligned sequences. The two nuclear localization signals (NLSs) in the DBD and IAD were indicated by dotted lines below the aligned sequences. The five conserved tryptophan (W) residues forming the 'tryptophan pentad-repeat' were indicated by triangle below the aligned sequences in the DBD. The identical and similar residues identified by the Clustal W program were indicated by black and gray, respectively. The accession numbers of IRF5 sequences are listed in **Table S1**.

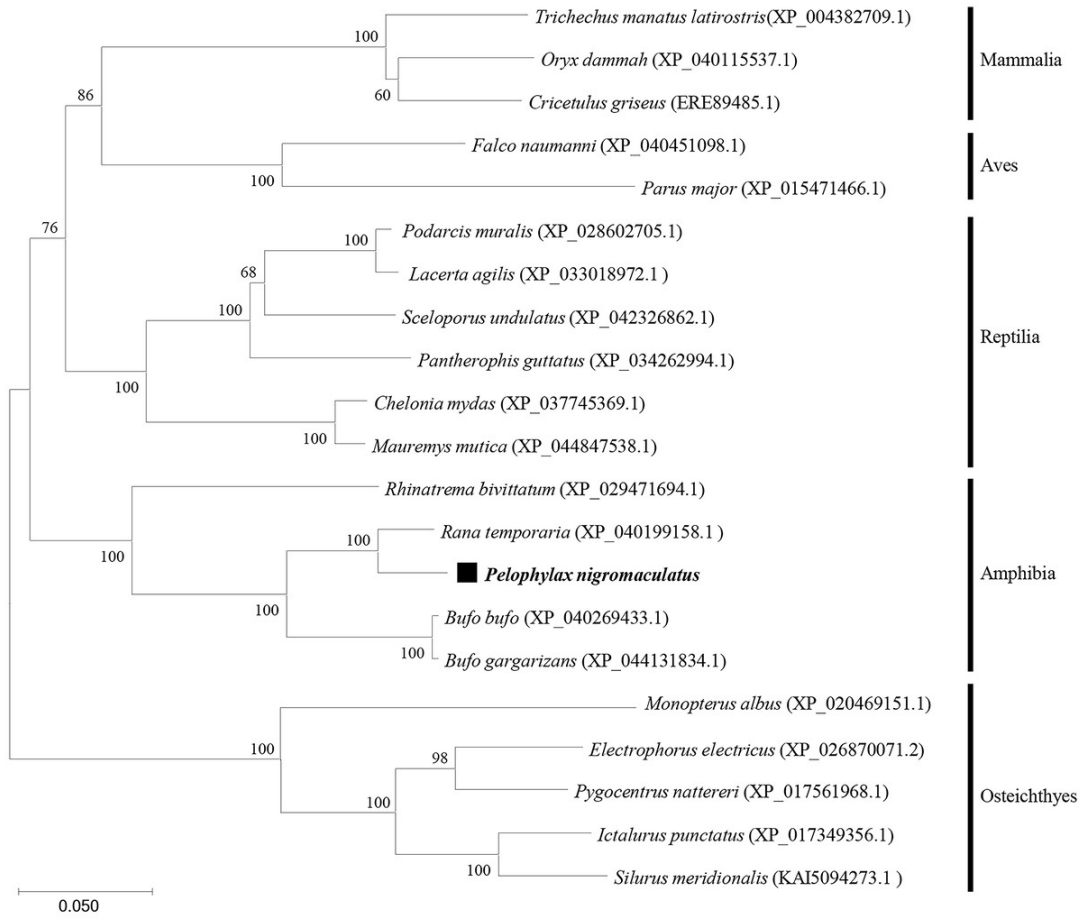

Figure 2. Phylogenetic relationship of IRF5 proteins. The tree is showed with 1000 replicates from the bootstrap test and the percentage of bootstrap are given next to the branches.

IRF5s amino acid sequence. In general, there were five groups in the phylogenetic tree with the Mammalia, Aves, Reptilia, Amphibia, and Osteichthyes with a clear genetic separation. In the Amphibia sub-tree, IRF5 from black-spotted frog was the most closely clustered with *R. temporaria* (Figure 2).

TERTIARY MODEL OF PNIRF5

The tertiary model of *Pn*IRF5 was built by Robetta using the RoseTTAFold modeling method. The tertiary structure of *Pn*IRF5 comprised three components that were relative independent in space, i.e., DBD, MR and part IAD, part IAD and VAD (Figure 3A). The DBD was composed of a three-stranded antiparallel β sheet and three α helices; it formed a helix-turn-helix domain. Moreover, five conserved tryptophan were all identified on the surface of DBD (Figure 3B, C). Two NLSs were distributed at the N- and C-terminal of *Pn*IRF5 protein (Figure 3A).

EXPRESSION LEVELS OF PNIR5 IN TISSUES

qPCR was performed to investigate mRNA expression levels of IRF5 in different tissues of black-spotted frog. As depicted in Figure 4, *Pn*IRF5 transcripts were ubiquitously expressed in all the tissues examined (e.g., the spleen, intestine, liver, muscle, brain, kidney, stomach, skin and lung tissues). The levels notably varied among different tissues. The relative expression of PnIRFF5 was significantly higher in kidney, intestine, lung, spleen, and skin than in other tissues ($p < 0.05$). No significant difference in *Pn*IRF5 mRNA expression was identified in heart, liver, muscle, and stomach ($p > 0.05$). Indeed, the maximum expression level of *Pn*IRF5 in the kidney was nearly twelvefold of the lowest expression level in the brain (Figure 4).

EXPRESSION OF PNIRF5 AFTER CHALLENGED WITH E. MIRICOLA

qPCR was performed to detect mRNA expression levels of *Pn*IRF5 in kidney, liver, and spleen tissues at different time points after *E. miricola* challenge. As depicted in Figure 5, 3 days after *E. miricola* challenged, a characteristic symptom of slight torticollis was identified in infection black-spotted frogs (Figure 5-A). The mRNA relative expression levels of *Pn*IRF5 in spleen, liver, and kidney displayed significantly up- or down-regulation post *E. miricola* challenge. For kidney, *Pn*IRF5 expression level was significantly up-regulated at the respective test time point in comparison with 0 days post-challenged. The expression level of *Pn*IRF5 in spleen

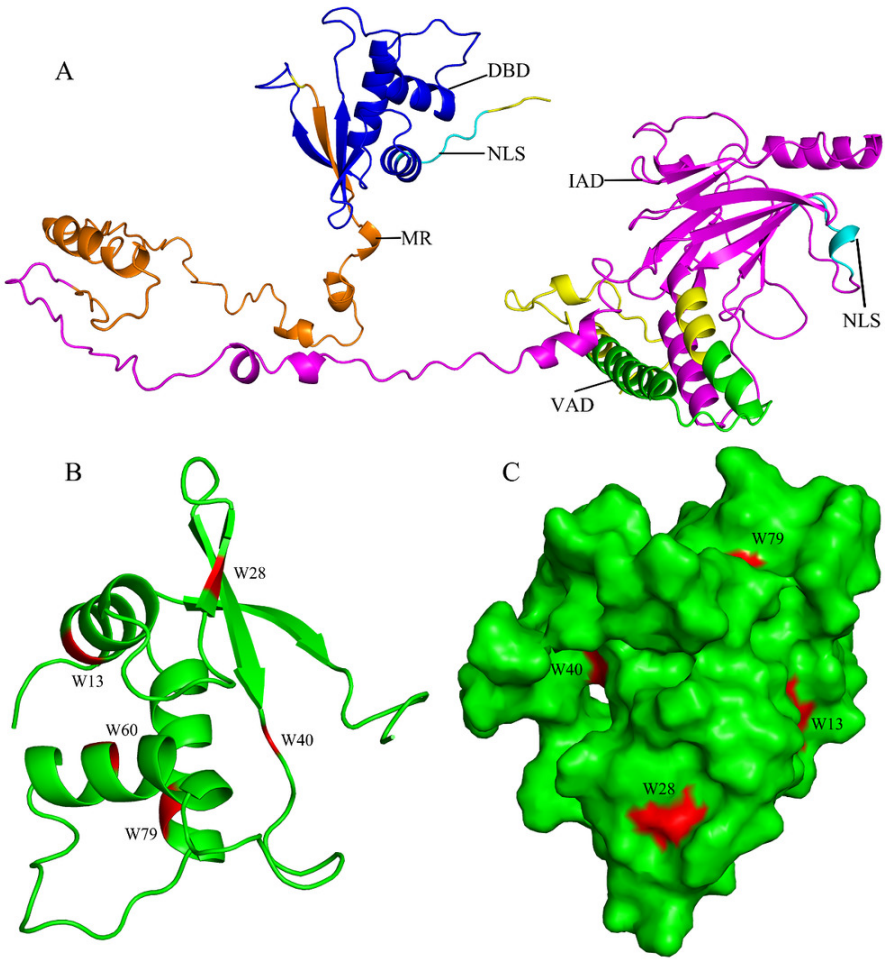

Figure 3. The tertiary structure and Connolly surfaces of *Pn*IRF5 were acquired by Robetta and the model was visualized using the PyMOL graphical user interface.

(**A**) The tertiary structure of *Pn*IRF5, DNA binding domain (blue), NLSs (cyan), MR (orange), IAD (magentas) and VAD (green). **(B and C)** The tertiary structure (B) and Connolly surfaces (C) of *Pn*IRF5 DBD domain, the five conserved tryptophan (W) residues in DBD were and marked with label and red.

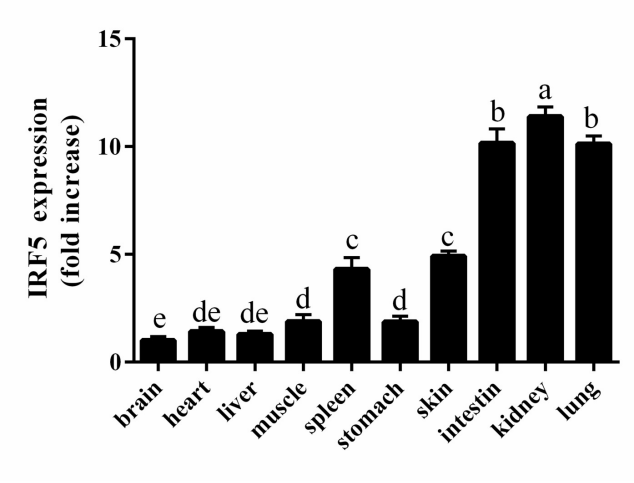

Figure 4. The expression patterns of *Pn*IRF5 in healthy black-spotted frogs.

The expression of *Pn*IRF5 were examined in different organs or tissues from black-spotted frog by qPCR relative to the reference gene 18S. Vertical bars represent the mean ± S.D. from three individual samples and difference letters indicate the significant difference between tissues (p <0.05).

and liver peaked at 3 days post-injection, and it was peaked at 2 days post-injection in kidney. Furthermore, the maximum expression level of *Pn*IRF5 in liver, spleen, and kidney was 1.80, 2.33 and 2.88 times that at time point 0 days, respectively. In comparison with 0 day post-challenged, the mRNA relative expression levels of *Pn*IRF5 were up-regulated with significance in kidney, liver, and spleen at 3 days after *E. miricola* challenge ($p < 0.05$).

DISCUSSION

Vertebrate IRF5 gene has been confirmed as the critical transcription factor for inducing type I interferon. At present, rare studies on IRF5 have been conducted in amphibian. In this study, the IRF5 gene cDNA sequence originated from black spotted frog, and its structure and expression character were explored initially. The full cDNA sequence of *Pn*IRF5 covered an ORF encoding a protein with 504 amino acids exhibiting the typical structural features of the IRF family.

As indicated by the amino acids sequence comparison, the *Pn*IRF5 exhibited an 80.79 - 93.85 % of similarity with other amphibians and a 48.73 - 61.26 % of similarity with

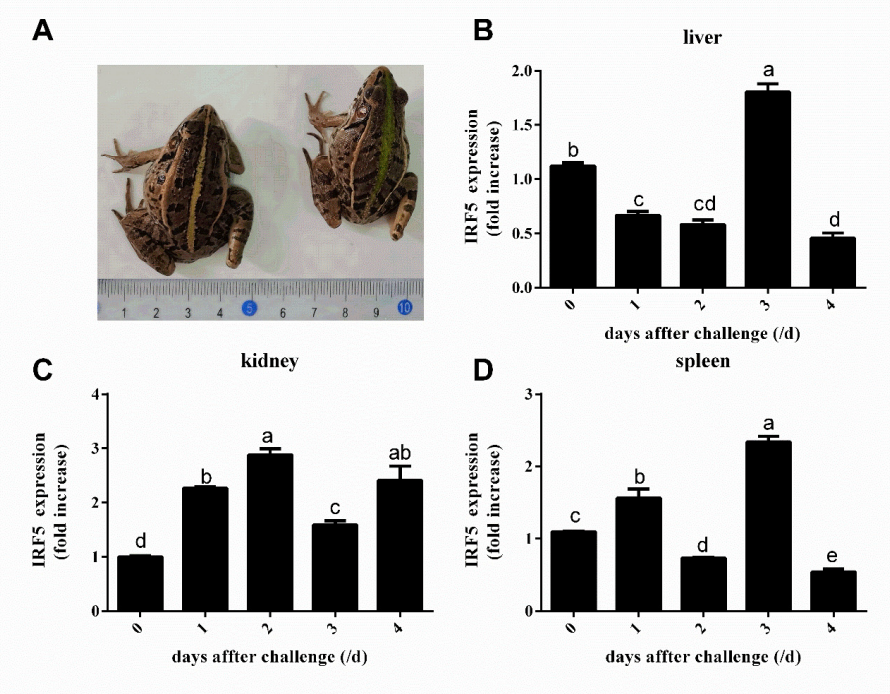

Figure 5. Expression of *Pn*IRF5 gene in the liver, kidney, and spleen tissues of black-spotted frogs after *E. miricola* infection(N=3).

(A) The characteristic symptoms of slight torticollis in black-spotted frogs after *E. miricola* infection. **(B)** The relative expression of *Pn*IRF5 gene in the liver. **(C)** The relative expression of *Pn*IRF5 gene in the kidney. **(D)** The relative expression of *Pn*IRF5 gene in the spleen. Vertical bars represent the mean ± S.D. from three individual samples and different lower-case letters above columns indicate significant differences between difference times after infection *E. miricola*. ($p < 0.05$).

other species, suggesting the main structure and function of IRF5 exhibited little diversity between species. *Pn*IRF5 contained a well-conserved N-terminal DBD of 104 amino acids, formed a helix-turn-helix domain, exhibiting five conserved tryptophan repeats, and served as essential domain to bind to IFN-stimulated response element (ISRE, A/GNGAAANNGAAACT) in the promoter region of target genes.[24,25] The analyzed tertiary structure suggested that five conserved tryptophan repeats were all on surface of DBD domain. Some previous research has confirmed that tryptophan repeats are a vital component for the protein that can function normally. The W401 residue in human immunodeficiency virus type-1 (HIV-1) reverse transcriptase (RT) Trp-motif takes on critical significance in RT dimerization,[26] the W401A mutants were defected for dimerization and devoid of RT activity.[27] Zhang[28] suggested that the Nanog tryptophan repeat region refers to the location of repression function of Nanog and represents a vital module of Nanog in fine-tuning the balance between self-renewal and differentiation. The contributions of tryptophan repeats in DBD of IRF5 remain unclear, which the elucidation of the immunological regulatory mechanism of IRF will be an interested research topic. The IAD domain of IRF5 in species showed lower conserved in comparison with DBD domain. The lower conserved IAD domain at the C-end results in a wide range of functional diversity of IRFs, which endows IRF family members with the ability to display differential transcriptional activity of different IFN genes or ISGs in different cell types or under different viral infection conditions.[6] IAD can mediate interaction with itself, other IRF family members, or other transcription factor family members, and regulate timely and appropriate expression of IFN gene in specific cell classes through synergism or antagonism.[24,29] *Pn*IRF5 also contains a VAD at C-terminal, VAD possesses many conserved serine residues, which may serve as virus-induced phosphorylation sites.[30] Phylogenetic analysis indicated that IRF5 from black-spotted frog was the most closely clustered with *R. temporaria*. Collectively, this evidence suggests that *Pn*IRF5 belongs to the IRF5 family member.

The tissue expression characteristics of IRF5 have been investigated most in the fish, and IRF5 was expressed in almost all examined tissues of the fish, whereas the tissue distribution of IRF5 was different in different fish.[31-35] In this study, the *Pn*IRF5 was primarily expressed in kidney, intestine, and lung and moderately expressed in spleen and skin, consistent with the fish species (*Danio rerio*, *Mycobacterium tuberculosis*).[36,37] The possible reason for the differential tissue distribution of IRF5 may be the diverse potential immune systems between Fishes and amphibians. The spleen and kidney serve as crucial immune organs in amphibians, which have a rich resident population of macrophages and lymphocytes. Furthermore, the lung, intestine and skin are vital mucosal immune tissues of amphibians. IRF5 was highly expressed in the above-mentioned tissues, suggesting that *Pn*IRF5 may take on crucial significance in the activity of the immune system in black spotted frog.

E. miricola is highly pathogenic to black spotted frog, and no cure has been reported for the control of its infec-

tion. The expression profiling of *Pn*IRF5 in three immune-associated tissues was examined to gain insights into the role of *Pn*IRF5 in response to the infection with *E. miricola*. After challenged with *E. miricola, Pn*IRF5 expression level all tended to be increased significantly in liver, spleen, and kidney. The similarity results were identified in spleen, head kidney, and liver of *Cyprinus carpio* L.[35] and *Cynoglossus semilaevis*,[34] IRF5 gene was significantly up-regulated upon LPS and *Vibrio harveyi* challenges, respectively. Furthermore, Pandey *et al*. suggested that after *Mycobacterium tuberculosis* infection, type I IFN expression can be stimulated through a pathway that is dependent on NOD2, RIP2, TBK1, and IRF5 in mice.[36] Notably, the up-regulated expression of IRF5 after *E. miricola* infected may be required to play a certain role in the immune response.

CONCLUSIONS

In this study, the *Pn*IRF5 genes of *Pelophylax nigromaculatus* was cloned with a coding sequence length of 1515 bp, encoding 504 amino acids. *Pn*IRF5 genes were expressed in all tested tissues, and the maximum expression was identified in the kidney. Under *E. miricola* stress, the maximum expression level of *Pn*IRF5 in the liver, spleen, and kidney was 1.80, 2.33 and 2.88 times that at time point 0 days at 3 d, 3 d, and 2 d, respectively, suggesting that *Pn*IRF5 participated in the immune response of *P. nigromaculatus* resistance to *E. miricola* infected.

ACKNOWLEDGMENTS

This research was funded by the Natural Science Foundation of Hunan Province (Grant no. 2023JJ30435 and 2022NK4150), the Research Project of Education Department of Hunan Province (Grant no. 22B0701 and 22B0691) and the National Natural Science Foundation of China (Grant no. 31972835).

AUTHOR CONTRIBUTIONS

Conceptualization: Ronghua Wang, Pinhong Yang;
Methodology: Ronghua Wang, Ke Li, Menglu Yan, Yan Kang, Shuqiong Li;
Formal analysis and investigation: Ronghua Wang, Qing Tan;
Writing - original draft preparation: Ronghua Wang;
Writing - review, and editing: Ronghua Wang, Pinhong Yang, Zhongyuan Chen;
Funding acquisition: Pinhong Yang;
Resources: Qing Tan, Hongchun Jin, Jinlong Wang;
Supervision: Pinhong Yang.

Submitted: April 25, 2023 CST. Accepted: May 24, 2023 CST.
Published: June 12, 2023 CST.

REFERENCES

1. Pellerin A, Yasuda K, Cohen-Bucay A, et al. Monoallelic IRF5 deficiency in B cells prevents murine lupus. *JCI insight*. 2021;6:141395. doi:10.1172/jci.insight.141395. PMID:34197340

2. Zhao X, Zhang Y. IRF-mediated regulation of IFN antiviral response in fish. *Journal of Fisheries of China*. 2021;45:1592-1604.

3. Huang B, Qi ZT, Xu Z, Nie P. Global characterization of interferon regulatory factor (IRF) genes in vertebrates: glimpse of the diversification in evolution. *BMC Immunol*. 2010;11(1):22. doi:10.1186/1471-2172-11-22. PMID:20444275

4. Nehyba J, Hrdličková R, Burnside J, Bose HRJr. A Novel Interferon Regulatory Factor (IRF), IRF-10, Has a Unique Role in Immune Defense and Is Induced by the v-Rel Oncoprotein. *Molecular and Cellular Biology*. 2002;22(11):3942-3957. doi:10.1128/mcb.22.11.3942-3957.2002. PMID:11997525

5. Stein C, Caccamo M, Laird G, Leptin M. Conservation and divergence of gene families encoding components of innate immune response systems in zebrafish. *Genome Biol*. 2007;8(11):R251. doi:10.1186/gb-2007-8-11-r251. PMID:18039395

6. Tamura T, Yanai H, Savitsky D, Taniguchi T. The IRF family transcription factors in immunity and oncogenesis. *Annu Rev Immunol*. 2008;26(1):535-584. doi:10.1146/annurev.immunol.26.021607.090400

7. Zhao X, Gong XY, Li YL, Dan C, Gui JF, Zhang YB. Characterization of DNA Binding and Nuclear Retention Identifies Zebrafish IRF11 as a Positive Regulator of IFN Antiviral Response. *The Journal of immunology*. 2020;205(1):237-250. doi:10.4049/jimmunol.2000245

8. del Fresno C, Soulat D, Roth S, et al. Interferon-β Production via Dectin-1-Syk-IRF5 Signaling in Dendritic Cells Is Crucial for Immunity to C. albicans. *Immunity*. 2013;38(6):1176-1186. doi:10.1016/j.immuni.2013.05.010

9. Hedl M, Yan J, Abraham C. IRF5 and IRF5 Disease-Risk Variants Increase Glycolysis and Human M1 Macrophage Polarization by Regulating Proximal Signaling and Akt2 Activation. *Cell Reports*. 2016;16(9):2442-2455. doi:10.1016/j.celrep.2016.07.060. PMID:27545875

10. Hu G, Mancl ME, Barnes BJ. Signaling through IFN Regulatory Factor-5 Sensitizes p53-Deficient Tumors to DNA Damage–Induced Apoptosis and Cell Death. *Cancer Research*. 2005;65(16):7403-7412. doi:10.1158/0008-5472.can-05-0583

11. Krausgruber T, Blazek K, Smallie T, et al. IRF5 promotes inflammatory macrophage polarization and TH1-TH17 responses. *Nat Immunol*. 2011;12(3):231-238. doi:10.1038/ni.1990

12. Paun A, Bankoti R, Joshi T, Pitha PM, Stäger S. Critical role of IRF-5 in the development of T helper 1 responses to Leishmania donovani infection. *PLoS Pathog*. 2011;7(1):e1001246. doi:10.1371/journal.ppat.1001246. PMID:21253574

13. Hedl M, Abraham C. *IRF5* Risk Polymorphisms Contribute to Interindividual Variance in Pattern Recognition Receptor-Mediated Cytokine Secretion in Human Monocyte-Derived Cells. *The Journal of Immunology*. 2012;188(11):5348-5356. doi:10.4049/jimmunol.1103319. PMID:22544929

14. Ryzhakov G, Eames HL, Udalova IA. Activation and Function of Interferon Regulatory Factor 5. *Journal of Interferon & Cytokine Research*. 2015;35(2):71-78. doi:10.1089/jir.2014.0023

15. Taniguchi T, Mak TW, Yanai H, et al. Integral role of IRF-5 in the gene induction programme activated by Toll-like receptors. *Nature*. 2005;434(7030):243-249. doi:10.1038/nature03308

16. Yang C, Liu L, Liu J, et al. Black carp IRF5 interacts with TBK1 to trigger cell death following viral infection. *Developmental & Comparative Immunology*. 2019;100:103426. doi:10.1016/j.dci.2019.103426

17. Park JK, Kim JB, Do Y. Reference Intervals in Combined Veterinary Clinical Examinations of Male Black-Spotted Pond Frogs (Pelophylax nigromaculatus). *Animals*. 2021;11(5):1407. doi:10.3390/ani11051407. PMID:34069152

18. Chang L, Zhao T, Zhao C, et al. Microbiomic and transcriptomic insight into the pathogenesis of meningitis-like disease in cultured Pelophylax nigromaculatus. *Aquaculture*. 2021;530:735736. doi:10.1016/j.aquaculture.2020.735736

19. Hu R, Yuan J, Meng Y, Wang Z, Gu Z. Pathogenic *Elizabethkingia miricola* Infection in Cultured Black-Spotted Frogs, China, 2016. *Emerg Infect Dis*. 2017;23(12):2055-2059. doi:10.3201/eid2312.170942. PMID:29148374

20. Lei XP, Yi G, Wang KY, et al. *Elizabethkingia miricola* infection in Chinese spiny frog (*Quasipaa spinosa*). *Transbound Emerg Dis*. 2018;66(2):1049-1053. doi:10.1111/tbed.13101

21. Trimpert J, Eichhorn I, Vladimirova D, et al. *Elizabethkingia miricola* infection in multiple anuran species. *Transboundary and Emerging Diseases*. 2020;68(2):931-940. doi:10.1111/tbed.13761

22. Wang Y, Ouyang J, Luo X, et al. Identification and characterization of novel bi-functional cathelicidins from the black-spotted frog (Pelophylax nigromaculata) with both anti-infective and antioxidant activities. *Developmental & Comparative Immunology*. 2021;116:103928. doi:10.1016/j.dci.2020.103928

23. Xu X, Lai R. The Chemistry and Biological Activities of Peptides from Amphibian Skin Secretions. *Chem Rev*. 2015;115(4):1760-1846. doi:10.1021/cr4006704

24. Antonczyk A, Krist B, Sajek M, et al. Direct Inhibition of IRF-Dependent Transcriptional Regulatory Mechanisms Associated with Disease. *Front Immunol*. 2019;10. doi:10.3389/fimmu.2019.01176. PMID:31178872

25. Furui J, Uegaki K, Yamazaki T, et al. Solution structure of the IRF-2 DNA-binding domain: a novel subgroup of the winged helix–turn–helix family. *Structure*. 1998;6(4):491-500. doi:10.1016/s0969-2126(98)00050-1

26. Mulky A, Sarafianos SG, Jia Y, Arnold E, Kappes JC. Identification of amino acid residues in the human immunodeficiency virus type-1 reverse transcriptase tryptophan-repeat motif that are required for subunit interaction using infectious virions. *Journal of Molecular Biology*. 2005;349(4):673-684. doi:10.1016/j.jmb.2005.03.057

27. Tachedjian G, Aronson HEG, de los Santos M, Seehra J, McCoy JM, Goff SP. Role of residues in the tryptophan repeat motif for HIV-1 reverse transcriptase dimerization. *Journal of Molecular Biology*. 2003;326(2):381-396. doi:10.1016/s0022-2836(02)01433-x

28. Zhang J. *Functional Analysis of the Role of the Nanog Tryptophan Repeat in ES Cells*. University of Edinburgh; 2016.

29. Chiang HS, Liu HM. The Molecular Basis of Viral Inhibition of IRF- and STAT-Dependent Immune Responses. *Front Immunol*. 2019;9:3086. doi:10.3389/fimmu.2018.03086. PMID:30671058

30. Bathige SDNK, Whang I, Umasuthan N, et al. Interferon regulatory factors 4 and 8 in rock bream, Oplegnathus fasciatus: Structural and expressional evidence for their antimicrobial role in teleosts. *Fish & Shellfish Immunology*. 2012;33(4):857-871. doi:10.1016/j.fsi.2012.07.017

31. Hu GB, Lou HM, Dong XZ, Liu QM, Zhang SC. Characteristics of the interferon regulatory factor 5 (IRF5) and its expression in response to LCDV and poly I:C challenges in Japanese flounder, Paralichthys olivaceus. *Developmental & Comparative Immunology*. 2012;38(2):377-382. doi:10.1016/j.dci.2012.06.001

32. Wickramaarachchi WDN, Wan Q, Lim BS, et al. Genomic characterization of interferon regulatory factor 5 from rock bream (Oplegnathus fasciatus) and its role in antiviral defense. *Fish & Shellfish Immunology*. 2014;37(2):256-267. doi:10.1016/j.fsi.2014.02.002

33. Xia J, Hu GB, Dong XZ, Liu QM, Zhang SC. Molecular characterization and expression analysis of interferon regulatory factor 5 (IRF-5) in turbot, Scophthalmus maximus. *Fish & Shellfish Immunology*. 2012;32(1):211-218. doi:10.1016/j.fsi.2011.10.021

34. Zhang J, Li YX, Hu YH. Molecular characterization and expression analysis of eleven interferon regulatory factors in half-smooth tongue sole, Cynoglossus semilaevis. *Fish & Shellfish Immunol*. 2015;44(1):272-282. doi:10.1016/j.fsi.2015.02.033

35. Zhu Y, Qi C, Shan S, et al. Characterization of common carp (Cyprinus carpio L.) interferon regulatory factor 5 (IRF5) and its expression in response to viral and bacterial challenges. *BMC Vet Res*. 2016;12(1):127. doi:10.1186/s12917-016-0750-4. PMID:27350041

36. Pandey AK, Yang Y, Jiang Z, et al. NOD2, RIP2 and IRF5 play a critical role in the type I interferon response to Mycobacterium tuberculosis. *PLoS Pathog*. 2009;5(7):e1000500. doi:10.1371/journal.ppat.1000500. PMID:19578435

37. Xiang Z, Dong C, Qi L, et al. Characteristics of the interferon regulatory factor pairs zfIRF5/7 and their stimulation expression by ISKNV Infection in zebrafish (Danio rerio). *Developmental & Comparative Immunology*. 2010;34(12):1263-1273. doi:10.1016/j.dci.2010.07.003

SUPPLEMENTARY MATERIALS

Supplementary material

Download: https://ija.scholasticahq.com/article/77752-characteristics-of-the-interferon-regulatory-factor-irf5-and-its-stimulation-expression-by-_elizabethkingia-miricola_-infection-in-black-spotted-frog/attachment/163610.pdf